

Supporting information for

Spinel/Perovskite Cobaltite Nanocomposites Synthesized by Combinatorial Pulsed Laser Deposition

Yan Chen^{†,‡,⊥}, Shuchi Ojha[§], Nikolai Tsvetkov^{†,¶}, Dong Hun Kim^{§,||}, Bilge

Yildiz^{*,†,‡,§}, C.A. Ross^{*,§}

[†]Laboratory of Electrochemical Interfaces, [‡]Department of Nuclear Science and
Engineering, [§]Department of Materials Science and Engineering, Massachusetts Institute
of Technology, Cambridge, MA02139, USA

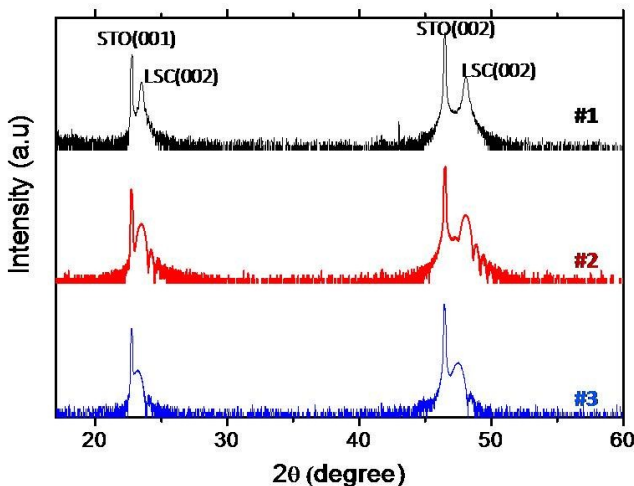


Figure S1. Comparison of the HRXRD 2θ - ω scans of LSC/CFO grown at 680 °C, with the fraction of CFO increasing from sample #1 to sample #3.

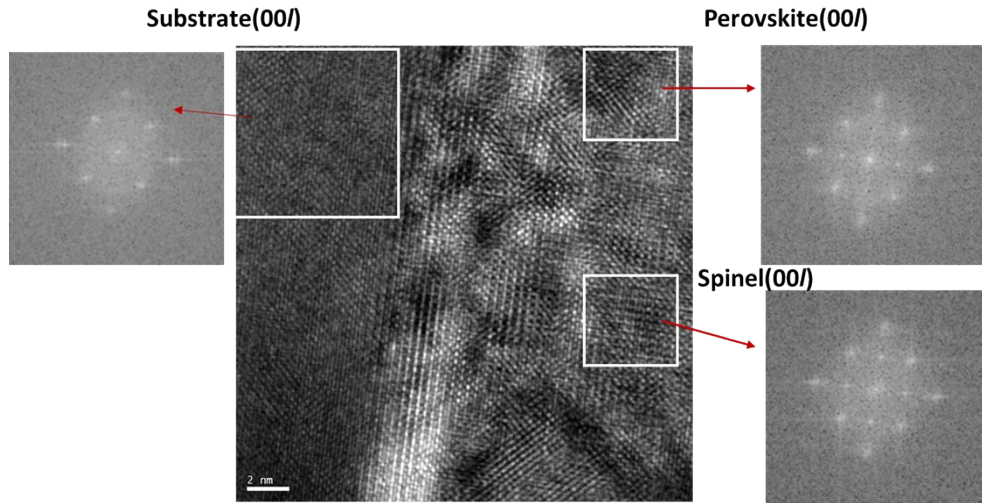


Figure S2. HRTEM image and corresponding Fast Fourier transform (FFT) pattern of LSC/CFO grown with 2 Hz laser frequency ($n_1=50$; $n_2=200$, $N=300$).

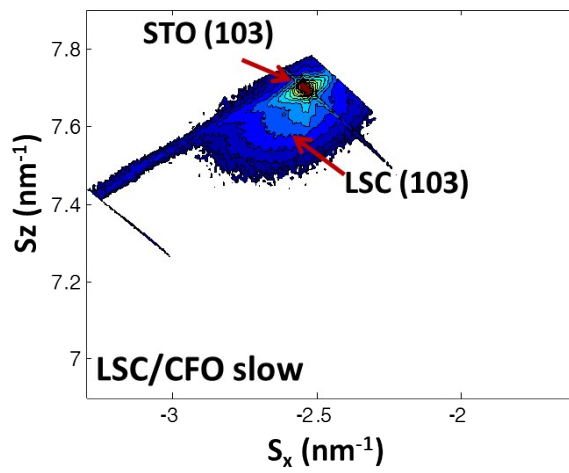


Figure S3. X-ray diffraction reciprocal space map of LSC/CFO on STO (100) grown at 600°C using 2 Hz laser rate

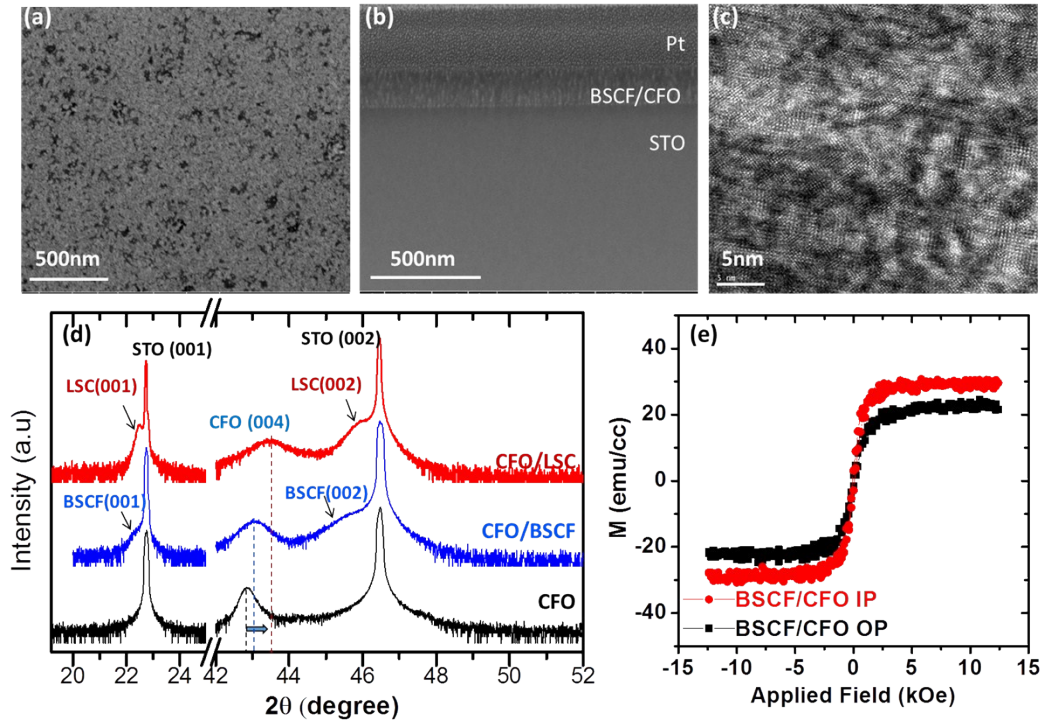


Figure S4: (a) Top surface and (b) cross sectional SEM image of BSCF/CFO nanocomposite structure grown at 600°C, 10 Hz, $n_1=50$; $n_2=200$, $N=300$; (c) HRTEM image of BSCF/CFO; (d) 2θ - ω scan of LSC/CFO, BSCF/CFO nano-composite and CFO single phase films; (e) In plane (IP) and out of plane (OP) magnetization loops of BSCF/CFO nanocomposite

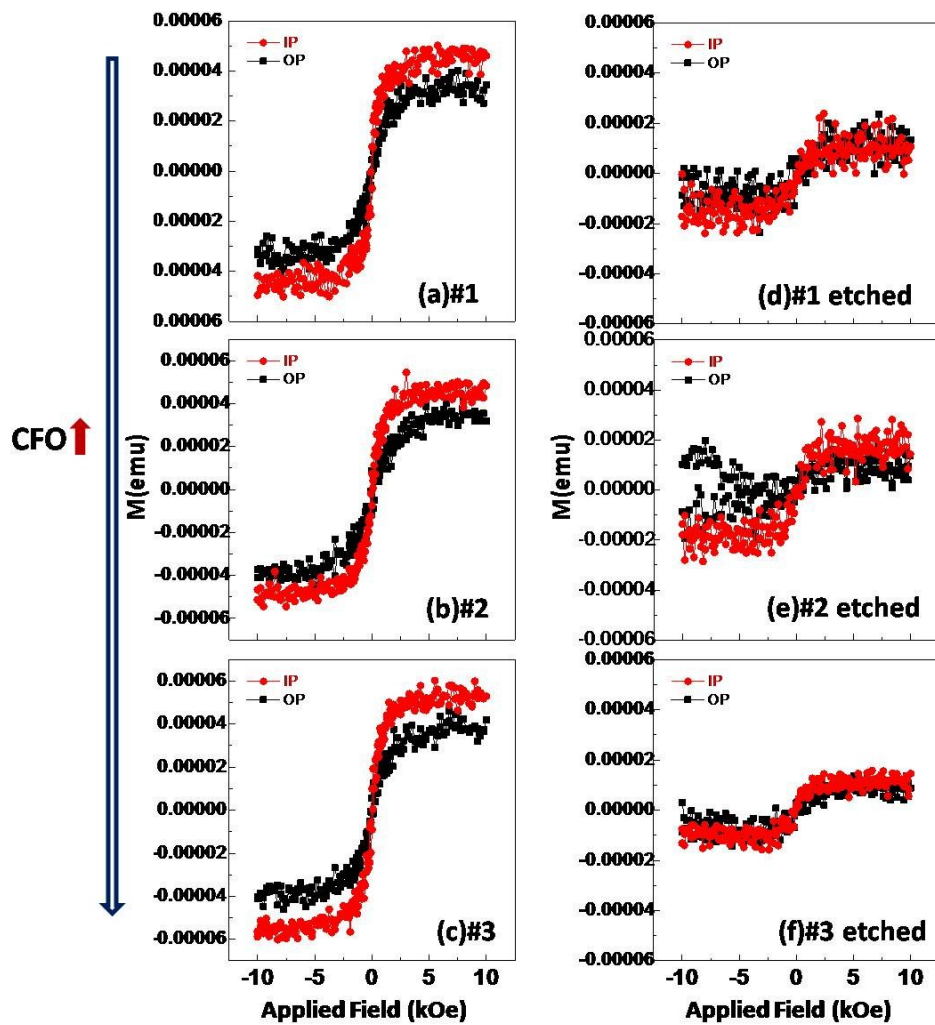


Figure S5: In plane (IP) and out of plane (OP) hysteresis loops of LSC/CFO nanocomposite grown at 680 °C, with the fraction of CFO increasing from sample #1 to sample #3 of Figure 2. (a-c) before and (d-f) after HCl etching.

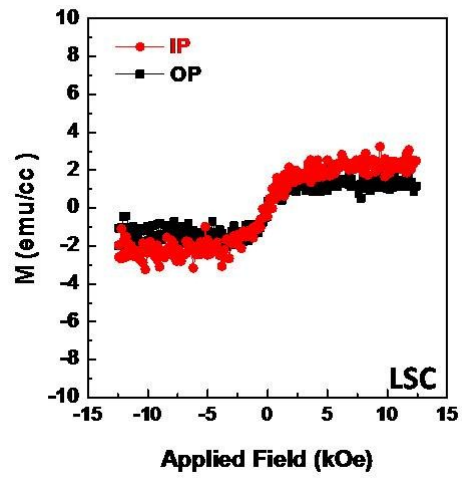


Figure S6: In plane (IP) and out of plane (OP) hysteresis loops of an LSC single phase film.